ANALYSIS OF HETEROGENEOUS NUCLEATION IN DUCTILE IRON

Simon N. Lekakh

Missouri University of Science and Technology, 1400 N. Bishop, Rolla, MO 65409

Keywords: Ductile iron, Graphite, Heterogeneous nucleation, 3-D quantitative technique

Abstract

A combination of an automated SEM/EDX analysis, a special 2D-3D converter of nodule size distribution, and adaptive thermal analysis were used for the study of heterogeneous nucleation in ductile iron. The special quenching technique was applied to increase probability to reveal non-metallic heterogeneous nuclei in small graphite nodules. Ternary diagrams were developed to compare statistics of oxide and sulfide compositions in graphite nodules and metal matrix. Thermodynamics of heterogeneous nucleation of graphite phase in Mg-treated cast iron is discussed based on the novel experimental data.

Experimental and Simulation Methods

Shape, size, quantity, and distribution of the graphite phase, developed during heterogeneous solidification in high carbon iron alloys (cast irons), are some of the most important microstructural parameters because the graphite phase influences the physical and mechanical properties of the final castings. In this article, developed approaches, including (i) an automated SEM/EDX analysis of graphite nodule heterogeneous nuclei chemistry[1-2] in quenched specimens and (ii) a special algorithm to convert two-dimensional to three-dimensional graphite nodule size distribution[3-5], were used in combination with (iii) an adaptive thermal analysis[6].

Heterogeneous nucleation statistic. Heterogeneous nucleation plays an important role in stable graphite eutectic solidification to avoid metastable cementite formation and associated shrinkage defects[7]. A vast variety of *FeSi*-based inoculants are used in ductile iron industrial practices. The thermo-chemistry of heterogeneous nucleation formation during melt inoculation was described by authors[8,9]. An experimental assessment of inoculation efficiency can be done on the basis of knowledge of heterogeneous nuclei chemistry. However, large graphite nodules (20-50 μm) in casting, relative to the size of potential nuclei (< 2 μm), makes it difficult to analyze potential nuclei chemistry in random section. Fig. 1 illustrates the calculated probability of visible nuclei in random section depending on graphite nodule size.

Quenched   Casting
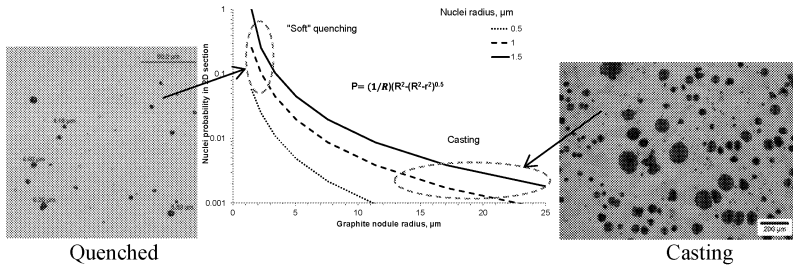
Fig. 1. Probability of nuclei view in random section of graphite nodules in cast structure and in quenched *Mg*-treated ductile iron.

A suggested technique for an evaluation of heterogeneous nuclei inside graphite nodules included two steps: (i) melt quenching to develop small graphite nodules (3-6 µm) with increased probability to reveal non-metallic heterogeneous nuclei and (ii) using automated SEM/EDX analysis to search potential nuclei in the center of small graphite nodules. In this study, samples were collected directly from the melt in the ladle after *Mg*-treatment using a submerged sampler with two internal steel chillers at 4 mm apart. A typical microstructure contained 3-6 mm diameter graphite nodules (Fig. 1).

Statistics of non-metallic inclusions were studied using an automated inclusion analyzer system, the Aspex PICA-1020. The applications of the automated analysis for control of non-metallic inclusions in iron matrix are described elsewhere[1,2]. In this study, the special search routine and rule files were developed to separately analyze non-metallic inclusions located in the metal matrix and inside graphite nodules. Fig. 2 shows the examples of different observed chemistries of heterogeneous nuclei inside small graphite nodules: (a) complex silicate with *MgS*, (b) *Si-Mg* oxide with small amount of *S*, and (c) complex *Mg-Ca* sulfide with *Mg-Si* oxide.

a)

b)

c)
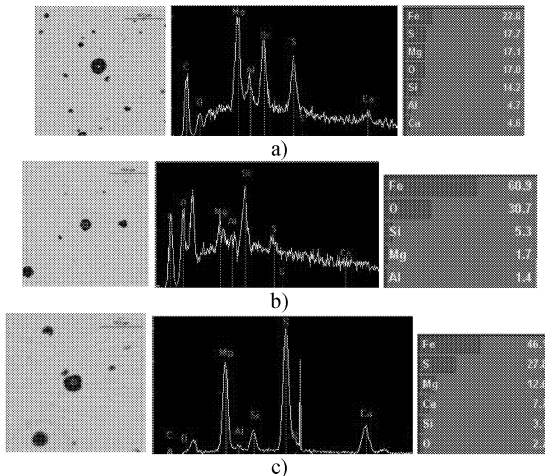
Fig. 2. Different types of non-metallic inclusions located inside graphite nodules.

Ternary diagrams were used (see below) to present experimental statistics of the graphite nuclei chemistry and for comparison to chemistry of inclusion located in the metal matrix.

Three dimensional quantitative analysis of ductile iron structure. Because micro-structure parameters obtained from the optical image of random planes have significant limitations[3,4], an automated SEM/EDX analysis was used to collect nodule size statistics in a random section. EDX analysis of each particle was used to separate the carbon containing phase from non-metallic inclusions. After that, two-dimensional graphite nodule diameter statistic (2D) was converted into three-dimensional spheres diameter (3D) statistic and volume population density methods using the suggested method[3,4].

Adaptive thermal analysis. ATAS (Novacast) thermal analysis was used for the determination of the set of solidification parameters which characterize inoculation efficiency[6].

Structure and Properties of Two Ductile Irons

It is well known that charge materials could effect on the chill tendency of produced ductile irons. Two ductile irons (Table 1) were melted in the laboratory 200 lbs induction furnace targeting the same basic chemistry (3.7 %C, 1.7 %Si); however, using different industrial charges to verify its effect on structure and properties of ductile irons. In both cases, melt was *Mg*-treated in the ladle by 1.6% alloy (*Fe*-46%*Si*-6%*Mg*-1%*Ca*) and inoculated by 0.3% of *Fe*-75%*Si*-1%*Al*-1%*Ca*.

Table 1. Casting chemistry in two experimental heats (wt. %).

Heat	C	Si	Mn	S	Cr	Ni	Ti	La	Mg
1	3.56	2.86	0.20	0.005	0.026	0.023	0.006	0.010	0.036
2	3.63	2.84	0.22	0.005	0.022	0.025	0.006	0.005	0.047

Adaptive thermal analysis of *Mg*-treated and inoculated melts from the ladle just before pouring castings (Fig. 2) showed that these two ductile irons had the large differences in solidification parameters, which typically are linked to nucleation efficiency[6] (highter TE_{low} and $GRF1$, lower recolecence R in Heat 1).
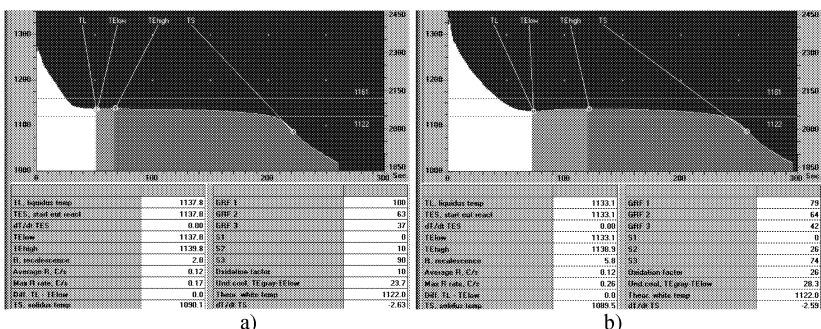
Fig. 3. Adaptive thermal analysis of Heat 1 (a) and Heat 2 (b).

Microstructure in step plates (Fig. 4) also showed significant differences in the number of graphite nodules and related structure of metal matrix. Heat 1 had larger nodules number and less ferrite in 30 mm casting section.

5 mm

30 mm

Heat 1   *Heat 2*
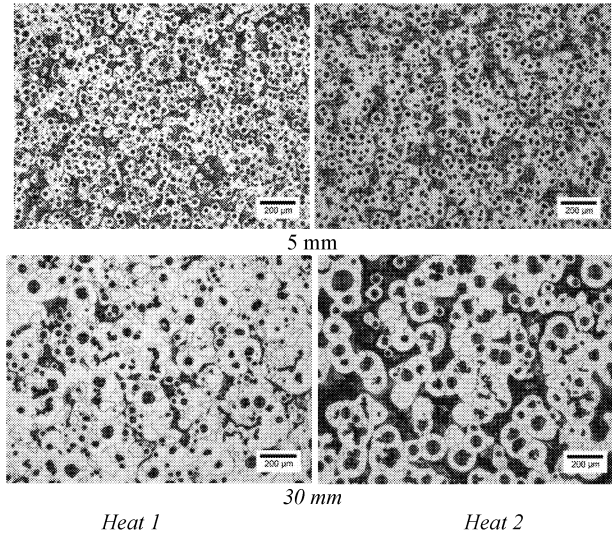
Fig. 4. Etched microstructure of castings in 5 mm and 30 mm thicknesses of step plate.

Three-dimentional statistic of graphite nuclei showed (Fig. 5) that the ductile iron in Heat 1 was better nucleated (highter nodule count in 1 mm^3 and less 3D-diameter) when compared to casting from Heat 2.

a)   b)
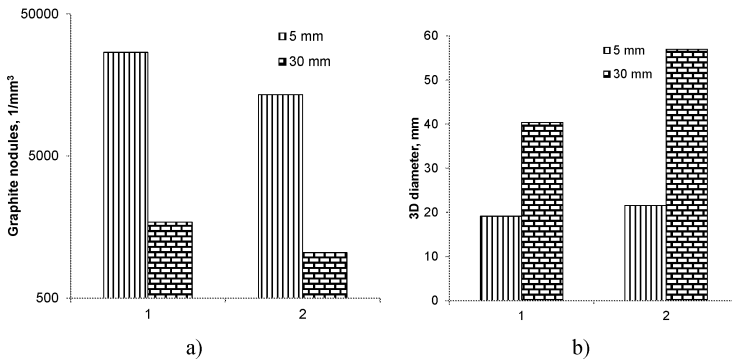
Fig. 5. Graphite nodules volume population density (a) and average 3-D diameter (b) in in step plates (5 and 30 mm thickness) from Heat 1 and Heat 2.

124

These ductile irons also have a different 3-D diameter statistic. Ductile iron from Heat 1 had bi-nodal 3-D diameter (Fig. 6a) and volume population density (Fig. 6b) distributions with a significant part of small graphite nodules.

a)   b)
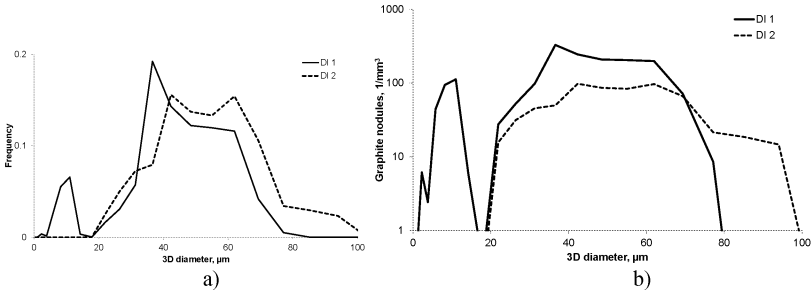
Fig. 6. Graphite nodule 3-D statistic: a) diameter and b) volume population density in 30 mm thickness step.

Described differences in graphite nodule dimensional statistic and metal matrix structure influenced on mechanical properties of these two ductile irons. Ductile iron from Heat 1 had higher elongation, toughness and, so-called", quality index Q=UTS^2*El.

Table 2. Mechanical properties of two ductile irons.

Ductile iron	UTS, KPa	YS, Kpsi	El, %	BHN	Q=UTS^2*El	CVN, ft-lbs
1	71.4	49.7	14.9	162	76.1	10.1
2	75.7	51.1	12.2	167	69.8	6.6

Analysis of Heterogeneous Nuclei

Two types of charge materials were used for production of the described ductile irons. In this article, the observed nucleation efficiency were linked to the actual chemistry of graphite nuclei. It could be observed that the majority of heterogeneous nuclei contained a complex of *Si-Mg-Ca* oxides and *Mg-Ca* sulfides. A limited amount of mono- *Mg* and *Ca* oxides and sulfides were found inside graphite nodules. Pure alumina was not found inside graphite nodules. The majority of inclusions in the metal matrix were complex *Mg-Si-Ca* oxide with significantly less concentration of *S* and *Ca* when compared to inclusions found inside graphite nuclei (Fig. 7).

125
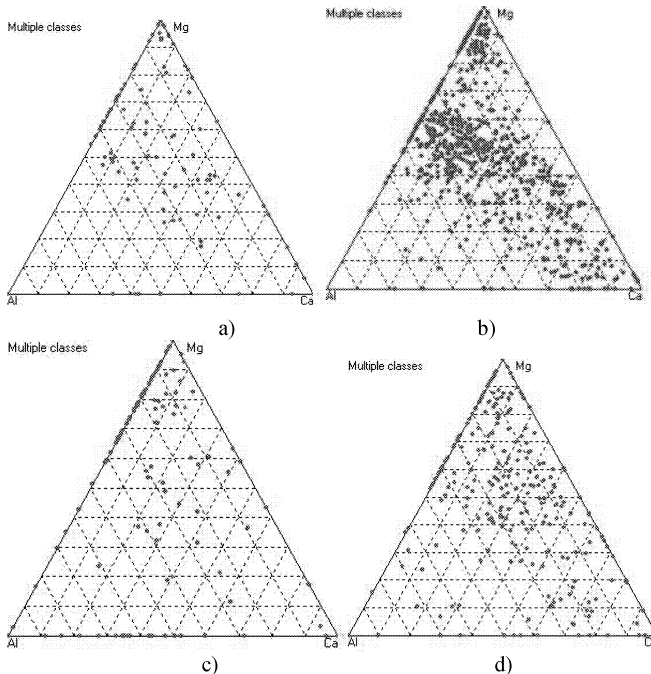
Fig. 7. Ternary diagrams of non-metallic inclusions located in metal matrix (a, c) and inside graphite nodules (b and d) in quenched specimens from Heat 1 (a, b) and Heat 2 (c, d).

Analysis showed significant partitioning of non-metallic inclusion between metal matrix and graphite nucleus (Table 3). Inclusions, which can be considered as potential heterogeneous nuclei, had a higher amount of Ca and S in both ductile irons. However, graphite nodules in ductile iron from Heat 1 showed more Ca and S when compared to Heat 2.

Table 3. Average chemistry of non-metallic inclusions in metal matrix and inside graphite nodules.

Heat	Location	Chemistry, wt. %				
		Mg	Al	Si	S	Ca
1	Nodules	22	10	41	19	12
	Matrix	25	5	49	17	4
2	Nodules	22	8	42	17	9
	Matrix	23	7	57	8	4

The thermodynamic simulation (FACTSAGE software) was used to predict the possible sequences of reactions which could take place in inoculant dissolution regions[8,9]. In these super-saturated regions, active elements, such as Mg, Ca, Si and Al, react with dissolved in the melt impurities S and O. In this article, different simulated scenarios included variations in a sulfur and calcium in Mg-treated melt. At very low residual S and Ca in the melt, MgO and more

complex oxides such as forsterite (Mg_2SiO_4) and merwinite ($Ca_3MgSi_2O_8$) could be formed at a high temperature 200-300^{0}C above ductile iron solidification interval (Fig. 8a). These inclusions can be easily agglomerated and floated out from the melt. From the stand point of stability of very fine inclusions in the melt, the scenario with some residual S and Ca in the Mg-treated melt looks more promising to enhance heterogeneous nucleation (Fig. 8b). The possible sequence of reactions will include early forming MgO and complex Mg-Si-O oxides (forsterite, for example) with sequential "coating" inclusions by sulfides (CaS) just before graphite eutectic solidification.
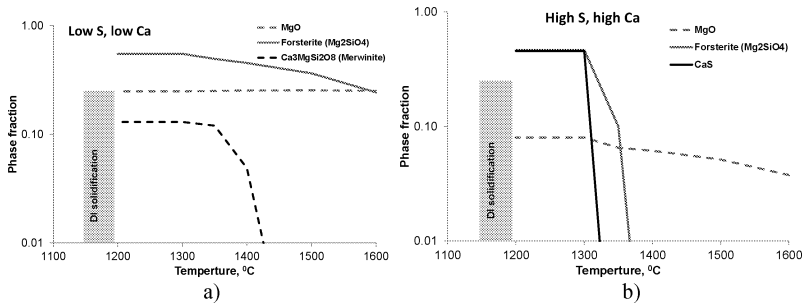
Fig. 8. Thermodynamic predictions of oxi-sylfide formation in Mg-treated melt with different levels of residual S and Ca.

Nucleation potential depends on several factors, including requirements of minimal interfacial energy between nuclei and growing phase which could be less for sulfides when compared to oxides. Important also is the temperature-time condition for inclusions precipitation in the melt: small and fresh formed inclusions with a minimal interfacial to graphite energy will have a higher graphite phase nucleation potential. Statistics of non-metallic inclusions inside graphite in the metal matrix showed a higher probability of complex ($Ca+S$)-containing inclusions inside graphite nodules. The experimental data support these thermodynamic considerations. Direct high resolution observation also showed the complex nature of heterogeneous nuclei in ductile iron[7]. Active heterogeneous nuclei provide continuous nucleation of spherical graphite during solidification, resulting in bi-modal three-dimensional graphite nodule distributions in the casting. Fig. 9 illustrates the effect of nuclei chemistry on the size of graphite nodules in "soft quenched" specimens. In all cases, S-Ca-contained graphite nodules had significantly larger diameters, which indicated evidence of early nucleation.
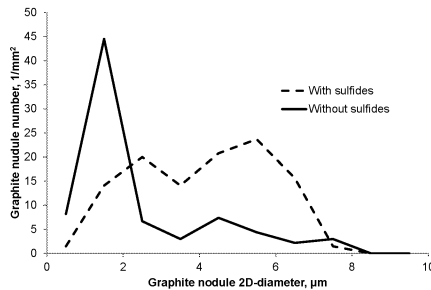
Fig. 9. Size distributions of graphite nodules with different types of nuclei.

Summary

The applied approaches including an automated SEM/EDX analysis of graphite nodule nucleation sites and a special algorithm to convert two-dimensional to three-dimensional graphite nodule size distribution were used to evaluate the effect of charge materials on heterogeneous nucleation in two ductile irons with similar main chemistries. It was shown that partitioning of Ca and S containing non-metallic inclusions between metal matrix and inclusions enclosed into graphite nodules takes place. Thermodynamic analysis was used to predict non-metallic inclusion formation sequences and correlate it with observed inclusion partitioning. Melting "history" plays a significant role in nucleation efficiency of inoculants and the methodology, described in this article, could be used for optimization of ductile iron treatment.

References

1. Singh V., Lekakh S., and Peaslee K., "Using Automated Inclusion Analysis for Casting Process Improvements", *Proceedings of the Steel Founders' Society of America 62th Annual Technical and Operating Conference*, Chicago (2008).
2. Lekakh S., Richards V., and Peaslee K., "Thermo-chemistry of Non-metallic Inclusions in DI", *The Carl Loper Cast Iron Symposium Proceedings*, AFS (2009).
3. Lekakh S., Qing, J., Richards V., Peaslee K., "Graphite Nodule Size Distribution in Ductile Iron", *AFS Proceedings* (2013).
4. Lekakh S., Thapliyal V., and Peaslee K., "Use of an inverse algorithm for 2d to 3d particle size conversion and its application to non-metallic inclusion analysis in steel", *AIST Proceedings* (2013).
5. Lekakh S., Harris M., "Novel Approaches to Analyze Structure of Ductile Iron", *Keith Millis Symposium on Ductile Cast Iron Proceedings*, AFS (2013).
6. Novacast: ATAS, http://www.novacast.se
7. Skaland T, "Nucleation Mechanism in Ductile iron", *Proc. AFS Cast Iron Inoculation Conference* (2005).
8. Lekakh S. and Loper C. R., "Improving Inoculation of Ductile Iron", *AFS Proceedings* (2003).
9. Lekakh S., Robertson D., and Loper C. R., "Thermochemistry and Kinetics of Iron Melt Treatment", *World Foundry Congress Proceedings*, UK (2006)